Journal of Catalysis **208,** 89–99 (2002)
doi:10.1006/jcat.2002.3530, available online at http://www.idealibrary.com on IDEAL®

A Theoretical Study of Hydrodesulfurization and Hydrogenation of Dibenzothiophene Catalyzed by Small Zeolitic Cluster

Xavier Rozanska,*,[1] Xavier Saintigny,* Rutger A. van Santen,*
Sylvain Clémendot,† and François Hutschka†

*Schuit Institute of Catalysis, Laboratory of Inorganic Chemistry and Catalysis, Eindhoven University of Technology, P.O. Box 513, 5600 MB Eindhoven, The Netherlands; and †TotalFinaElf, Centre Européen de Recherche et Technique, Département Chimie des Procédés, B.P. 27, 76700 Harfleur, France

Received August 23, 2001; revised November 5, 2001; accepted December 28, 2001

Hydrodesulfurization of dibenzothiophene (DBT) by an unpromoted acidic zeolite has been theoretically studied using density functional theory method with the cluster approach. Different reactions have been investigated. The direct hydrodesulfurization of DBT and the hydrodesulfurization of hydrogenated DBT are described. Furthermore, aromatic hydrogenation has been considered. A detailed description of the intermediates and transition states corresponding to the different reaction pathways is provided. The elementary DBT cracking reaction, which leads to the formation of biphenylthiol, is the most difficult reaction in the DBT hydrodesulfurization reaction pathway. Once this step has been achieved, sulfur removal becomes favorable. However, aromatic hydrogenation appears to be a more favorable reaction than DBT cracking. It is predicted that hydrogenation will preferentially take place. The ring cracking activation energies of hydrogenated DBT are on the same order as those of aromatic hydrogenation.

Key Words: **Brønsted acid site; zeolite; DFT calculations; quantum chemistry; hydrodesulfurization; desulfurization; cracking; hydrogenation; aromatic; DBT.**

1. INTRODUCTION

The hydrotreating reaction, which is used extensively both for the conversion of heavy feedstocks and to improve the quality of the final product, represents one of the most important catalytic processes in the petroleum refining industry (1, 2). This process mainly aims at removing heteroatoms, such as sulfur, oxygen, and metals, in order to protect catalysts in downstream operations. Today, the greater needs for processing heavier feedstocks enhance the pressure to improve hydrotreating processes, as both oil supplies and demand in fuel oil should decline. Moreover, worldwide environmental legislation places increasingly severe restrictions on transportation fuels (1, 2). Hence, processes such as deep desulfurization and dearomatization will become more and more important for providing environmentally friendly fuel.

Sulfur compounds present in diesel fuel can be divided into two groups displaying different hydrodesulfurization (HDS) activities (2, 3). Compounds such as thiols, sulfides, and thiophenes form a first group, whereas thiophenic polyaromatic molecules form the second. The distinction between these two groups relates to the relative activity of the molecules with respect to hydrodesulfurization. The molecules of the first group do not cause problems in industrial hydrodesulfurization. Hence, emphasis has been placed on understanding of the reactivity and hydrodesulfurization mechanisms of benzothiophene (BT) and dibenzothiophene (DBT) in the past decade (1–6). Alkylated DBTs are particularly resistant to HDS, especially when alkylated in the 4 and 6 positions. Technical solutions that facilitate hydrodesulfurization of alkylated DBTs must be considered in order to enhance deep desulfurization of diesel fuel. This can be achieved by two different means: the first consists in the modification of the HDS reactor parameters (i.e., H_2 partial pressure, feedstock composition, and number of reaction stages); the second involves the use of new and more efficient catalysts (1–6). The development of catalysts with enhanced HDS activity is a more attractive approach, as any modification of the technological process requires capital investment.

Hydrocracking catalysts often consist of a sulfidic Ni–Mo or Ni–W phase dispersed over a zeolite support (1, 2, 7, 8). Extensive studies have been performed on such metal sulfide catalysts in the past 10 years (1–8). Interestingly, it appeared that the removal of sulfur from hydrocarbons could also be catalyzed by pure zeolites (9–12). Several authors have experimentally demonstrated the activity of acidic or cation-exchanged zeolites (9–15).

Vrinat *et al.* (9) observed that hydrodesulfurization of DBT can be achieved by either H- or Na-Y zeolites. They reported, moreover, a synergetic effect between Mo and H-Y, without the requirement of a sulfidation

[1] To whom correspondence should be addressed. Fax: 31 40 245 5054. E-mail: tgakxr@chem.tue.nl.

0021-9517/02 $35.00

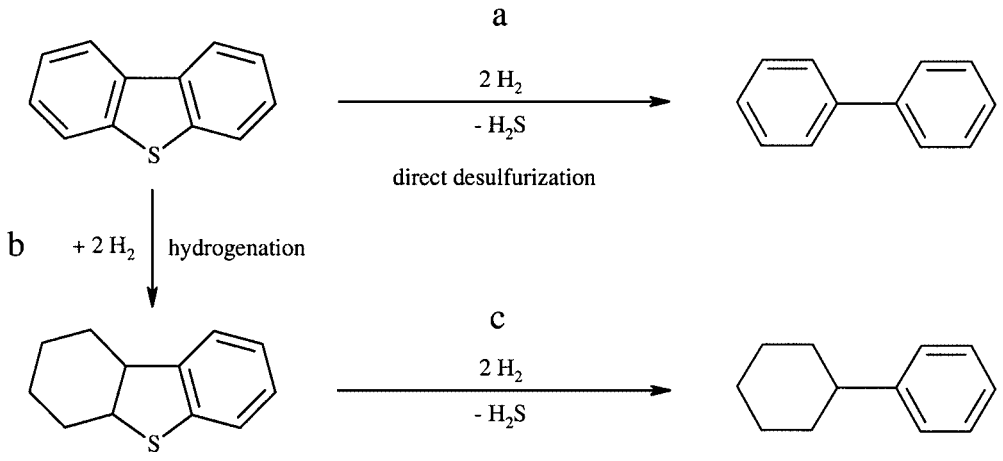

SCHEME 1. The main reaction routes for hydrodesulfurization of DBT.

pretreatment, which led to an important increase of the hydrodesulfurization rate. Cid *et al.* (10) obtained the same result in the case of ZSM-5. Welters *et al.* (11, 12) considered H-, Na-, and Ca-exchanged zeolite catalysts with and without Ni, Mo, or Co and showed that the HDS activity increases linearly by increasing the acidity, supporting the idea of the existence of a synergetic effect between the sulfidic and the zeolitic catalysts. In previous theoretical studies, we analyzed the thiophene hydrodesulfurization reaction catalyzed by acidic and Li-exchanged zeolite catalyst sites (13, 14). Furthermore, the effect of the thiophene prehydrogenation reaction was also investigated (14). The result of these studies, was that the presence of H_2 is mandatory for achieving the desulfurization reaction. This agrees with the experimental studies of Yu *et al.* (15).

The aim of the present study was to analyze unpromoted acidic zeolite pathways of DBT HDS. Two different reaction pathways are possible in conventional HDS (see Scheme 1) (3, 4). One reaction pathway involves direct sulfur removal, whereas the other occurs after the prehydrogenation reaction of at least one aromatic ring of DBT prior to C–S bond breaking. We will first consider the full desulfurization of DBT via the direct route (a in Scheme 1) and then analyze the hydrogenation reaction of aromatic species catalyzed by an acidic zeolite-active site (b in Scheme 1). Benzene was used as a small-scale model of aromatics for this purpose. Finally, we will investigate the initial step of the hydrodesulfurization of hydrogenated DBT that leads from hexahydrodibenzothiophene to cyclohexyl-2-benzenethiol species (c in Scheme 1).

In this study, for comparative purposes, we used a methodology similar to that used in previous studies (13, 14). The zeolite catalyst is modeled by a small cluster, a molecular fragment terminated by H atoms. This method, known as the cluster approach, has been successfully used for many years to describe zeolite-catalyzed reactions (13, 14, 16, 19). The drawback of this approach is that the zeolite crystal framework is not described (16–19). However, the effect of the zeolite framework on the course of the reaction is now rather well understood (19–25), and cluster approach calculations are revealed as an elegant method that allows a qualitative description of reaction mechanisms (19, 24).

The more important consequence of the nondescription of the zeolite framework is that activation energies obtained with the cluster approach are usually overestimated. The electrostatic stabilization of the carbocationic nature of transition states by the zeolite framework oxygen atoms can be quite significant and, as previously observed, can decrease computed activation energies by 10 to 30% (20–25). Despite this energetic stabilization, the geometries of transition states and intermediates were observed to be only slightly affected compared to cluster results (19, 24).

The zeolite framework electrostatic contribution increases the carbocationic nature of transition states. For instance, Vollmer and Truong (20), in their DFT study of the H exchange of methane with H-Y zeolite, reported that the inclusion of the zeolite crystal Madelung potential shifted the relative locations of the exchanging protons at the transition-state geometry toward a more carbocationic system. The characteristic distances of the transition state were altered by 0.05 to 0.13 Å.

The zeolite framework stabilization has been shown not to affect the relative energies of neutral species (21). In transition states (TS), it is dependent not only on the zeolite structure but also on the location of the TS within the zeolite micropore, as zeolite electrostatic contributions are mainly of a short-range nature (20–26).

In the case of our small cluster calculations, we did not aim to describe the zeolite framework. Therefore, the reaction energies we present are not specific for any zeolite but correspond to reactions catalyzed by a zeolitic Brønsted acid site in the absence of zeolite framework dependence. Such a situation is experimentally encountered with large-pore zeolites, or with mesoporous zeolites when

the reactant is DBT. As recently demonstrated by Sato *et al.* (27), the mesopore surface of H-zeolite (i.e., H-Y) plays an important role in the hydrodesulfurization of heavy oils. Mespore surfaces either exist in low-crystallinity zeolites or can be generated upon chemical treatment (27).

Despite the shortcuts of the cluster approach method, we recently demonstrated that a very good qualitative description of the energy and geometry data is obtained when cluster approach data are compared to those of a more elaborate model for which the zeolite framework is considered (i.e., periodic DFT calculations) (19, 24). In these studies of aromatic isomerization, we observed that the reaction energy ordering is altered by less than 5 kJ/mol between the cluster approach method and the periodic method. Quantum-chemical cluster approach calculations provide the opportunity of identifying the reaction mechanisms that are involved in the hydrocracking of DBT and of qualitatively predicting whether and how hydrogenation affects this reaction.

2. METHODS

All calculations were performed with Gaussian98 (28) using the hybrid DFT B3LYP method (29–31). In zeolitic systems, this method has been shown to provide results as good as or better than MP2 calculations (32–33). The basis set 6–31g* was used for all atoms. The basis set superposition error was tested for some systems and found to be around 10 kJ/mol for both adsorption and activation energies (14, 34–36). These reasonable errors are in agreement with the values obtained in other studies (32, 33).

The zeolitic cluster model that was used constitutes 19 atoms ($Al(OSiH_3)_2(OHSiH_3)(OH)$) containing four tetrahedral atoms, and is therefore called T4. Cluster models such as $Al(OSiH_3)(OHSiH_3)(OH)_2$ are called T3 (13).

Geometry optimization calculations were carried out to obtain a local minimum for reactants, adsorption complexes, and products and to determine the saddle point for TS. The frequencies were computed using analytical second derivatives to ensure that the stationary point exhibits the proper number of imaginary frequencies: none for a minimum and one for a TS (first-order saddle point). Zero-point-energy (ZPE) corrections, which correspond to the summation of $\frac{1}{2}h\nu_i$ for each normal vibration, were calculated for all optimized structures. All energies presented hereafter are ZPEs.

3. RESULTS AND DISCUSSION

As already mentioned, the HDS of DBTs can proceed via two different reaction pathways (see Scheme 1), and hydrogenation reactions play a role in one of these. It is well established that pure zeolite catalysts can be used for hydrogenation (37, 38). In the first part of this section, we will focus on the direct hydrodesulfurization pathway (see a in Scheme 1). A detailed description of the mechanisms for DBT is provided and compared to the results obtained in the case of thiophene HDS (13, 14). We will analyze the hydrogenation reaction of benzene and whether hydrogenation can compete with HDS reactions in the second part of this section. Finally, we will analyze the cracking reaction of hydrogenated DBT.

3.1. DBT Thiophenic Ring Cracking

The theoretical study using the cluster approach of the direct hydrodesulfurization of DBT (reaction a), which leads with H_2 to the formation of biphenyl and H_2S, is discussed. The mechanism of DBT direct hydrodesulfurization consists of two consecutive parts. The first concerns thiophenic ring cracking. Protonation of the product leads to the formation of phenyl-2-thiophenol (see Fig. 1a). The other part of the mechanisms deals with the hydrodesulfurization of biphenylthiol, which results in the formation of biphenyl and H_2S (see Fig. 1b).

The reaction is initiated from DBT physisorbed to the molecular cluster. It has been reported that thiophene derivatives adsorb to the zeolite proton via the $\eta^1(S)$ adsorption mode in IR spectroscopy studies (39, 40). We used these observations to model the geometry of physisorbed DBT and performed a full optimization of the system (see Int1a in Figs. 1a and 2). The distance between the thiophenic S atom and the zeolite model proton is $SH_a = 2.28$ Å, which induces a weakening of the O–H bond ($O_1H_a = 0.97$ to 0.99 Å). The interaction energy of DBT with the Brønsted acid site is $E_{ads} = -28$ kJ/mol.

After adsorption of DBT, the thiophenic C–S bond cleavage occurs (see TS1a in Figs. 1a and 2 and Table 1). This reaction appears to be induced by a Lewis base oxygen atom as observed in the case of thiophene (14). The C–S bond cleavage is favored by the correlative formation of a O–C bond, whereas protonation of the sulfur follows afterwards. The activation energy of this step is $E_{act} = 288$ kJ/mol, which is around 60 kJ/mol higher than that in thiophene molecule cracking (13, 14).

In this study, as in one of our previous studies (14), we used a T4 cluster to model the zeolite catalytic site. This cluster model is more suitable than a T3 cluster and allows the modeling of three oxygen atoms with the same correct electronic distribution as that found in zeolite (16–18). This is especially important because, as can be seen in Fig. 2 and later figures displaying the geometries of the computed structures, complex interactions exist between the DBT molecule and the zeolitic cluster. No fewer than three zeolitic oxygen atoms can get involved in these interactions. The activation energies of thiophene cracking catalyzed by T3 and T4 cluster models are 222 and 226 kJ/mol, respectively. The two cluster models display different acidic and basic strengths, but the activation energy of the thiophene cracking did not appear to be affected (13, 14).

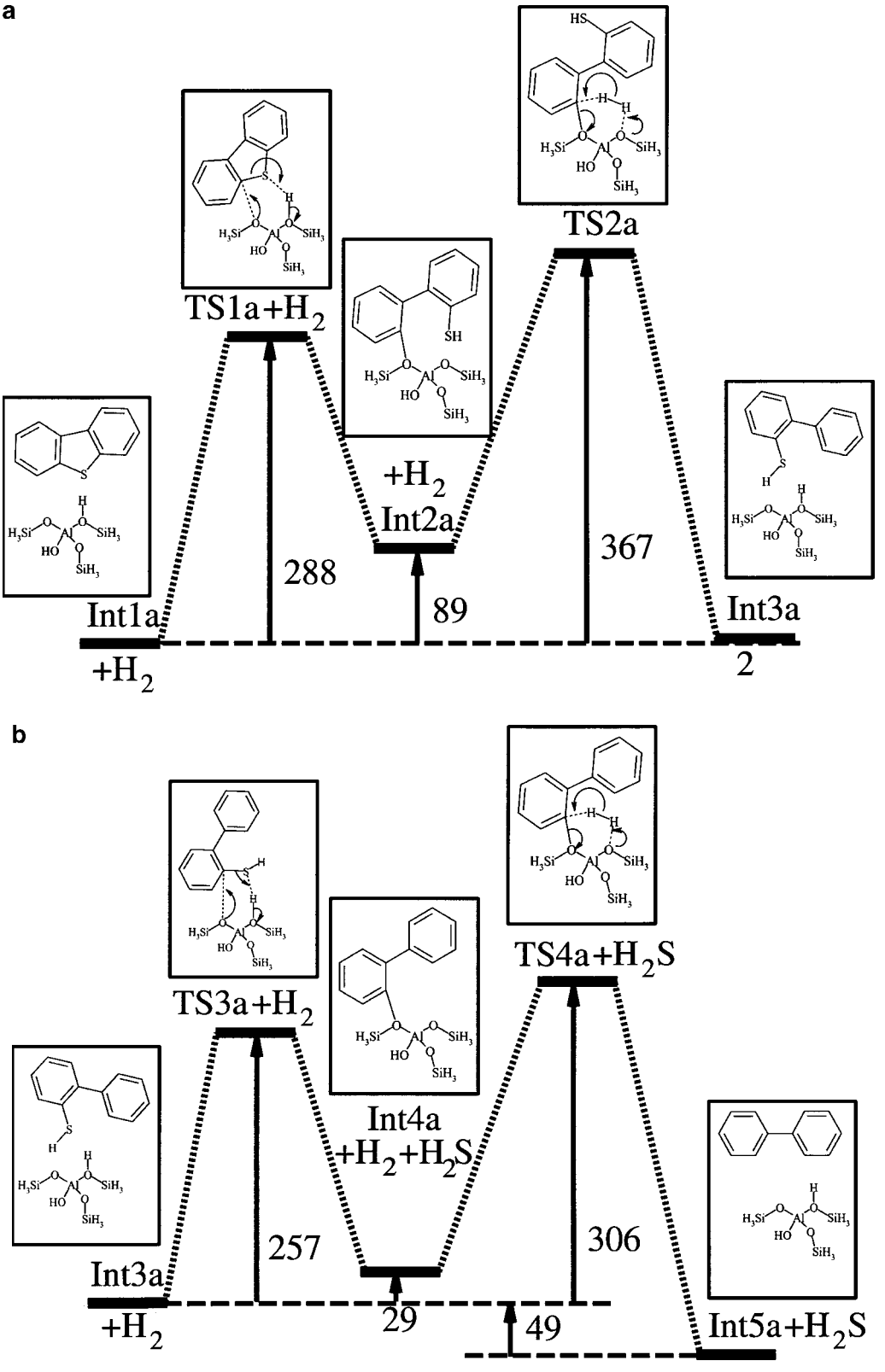

FIG. 1. (a) Reaction energy diagram of DBT thiophenic ring cracking catalyzed by an acidic zeolitic cluster (in kJ/mol). (b) Reaction energy diagram of biphenylthiol desulfurization catalyzed by an acidic zeolitic cluster (in kJ/mol).

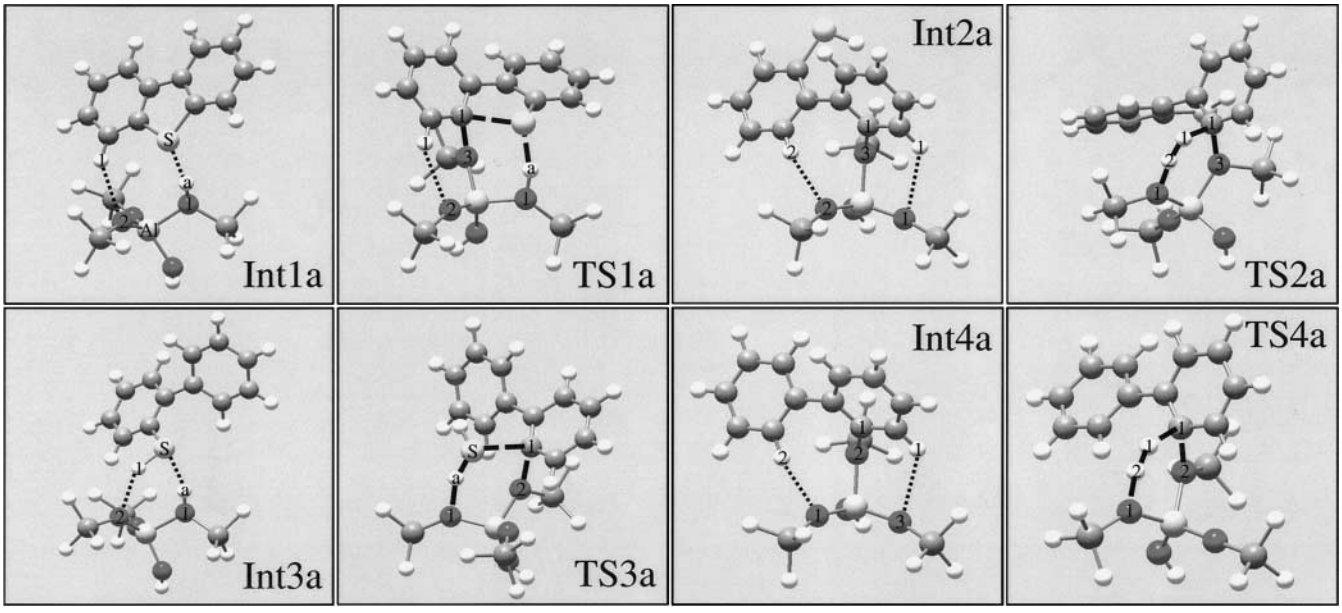

FIG. 2. Geometries of the intermediates and transition states in the thiophenic ring cracking and desulfurization of DBT catalyzed by an acidic zeolitic cluster.

After this step, a thiol-phenoxy species is obtained (see Int2a in Figs. 1a and 2). This intermediate is not very stable; however, it is actually more stable than its equivalent in the case of thiophene, which has an energy level 100 kJ/mol above that of physisorbed thiophene (13, 14). The reason for this slightly higher stability presumably originates from the existence of interactions between phenoxy intermediate hydrogen atoms and cluster oxygen atoms ($H_1O_1 = 2.79$ Å, and $H_2O_2 = 2.51$ Å). The C_1O_3 bond length is 1.41 Å. The alkoxy bond length was also 1.41 Å in the case of thiophene (13–14).

Next to this intermediate, one could consider two different reaction routes as in the case of thiophene (13). Without the assistance of H_2, the phenoxy intermediate can backdonate a proton to the cluster, leading to the formation of a benzyne intermediate. These species are, however, very unstable and are therefore unlikely to be formed under the experimental conditions usually required to achieve this reaction (41, 42). Only the reaction route that proceeds with the assistance of H_2 can be followed.

The adsorption complex of H_2 in Int2a could not be obtained, as all attempts to optimize such a structure led to H_2 desorption. This is because DFT methods cannot accurately describe the weak Van der Waals interaction (23, 43–46). Therefore, the activation energy barrier will be referred to the state where H_2 does not interact with the cluster

TABLE 1

Main Geometry Parameters of the Transition States in the Hydrodesulfurization of DBT Catalyzed by a T4 Acidic Zeolite Cluster[a]

TS1a		TS2a		TS3a		TS4a	
AlO_1	1.84	AlO_1	1.81	AlO_1	1.77	AlO_1	1.81
AlO_3	1.84	O_1H_2	1.29	O_1H_a	1.71	O_1H_2	1.32
O_1H_a	1.10	H_2H_1	0.96	H_aS	1.39	H_2H_1	0.95
H_aS	1.79	H_1C_1	1.38	SC_1	2.39	H_1C_1	1.38
SC_1	2.43	C_1O_3	1.64	C_1O_2	2.01	C_1O_2	1.74
C_1O_3	1.81	O_3Al	1.89	O_2Al	1.85	O_2Al	1.86
O_1H_aS	163.2	AlO_1H_2	99.9	O_1H_aS	160.1	AlO_1H_2	99.0
O_3C_1S	88.5	$O_1H_2H_1$	159.5	H_aSC_1	105.8	$O_1H_2H_1$	156.9
$H_aSC_1O_3$	−15.9	$H_2H_1C_1$	141.3	SC_1O_2	88.4	$H_2H_1C_1$	143.8
		$H_1C_1O_3$	89.4	$O_1SC_1O_2$	1.0	$H_1C_1O_2$	86.7
		C_1O_3Al	131.3			C_1O_2Al	124.8

[a]Distances in Å and angles in degrees. The labels that are used to design the transition states in this table are described in Fig. 2.

(13, 47, 48). The interaction energy of H_2 with the zeolite oxygen atoms is on the order of 10 kJ/mol (13, 47, 48).

The geometry of the transition state is shown in Figs. 1a and 2 (see TS2a). The dissociating H_2 molecule bridges between the carbon that was bonded to a zeolitic oxygen atom and the zeolitic oxygen atom to which the hydrogen atom will bond (see Table 1). All the atoms that are involved in this transition state belong to almost the same plane ($O_3C_1H_1H_2 = -10.6°$, and $O_1H_2H_1C_1 = 3.7°$). This hydrogenation reaction step is as difficult to achieve as DBT cracking ($E_{act} = 278$ kJ/mol with respect to Int2a, and 367 kJ/mol with respect to physisorbed DBT). In the case of thiophene (13), the activation energy for this step is around $E_{act} = 320$ kJ/mol with respect to physisorbed thiophene.

TS2a leads to the formation of biphenylthiol. The energy of physisorbed biphenylthiol to the zeolite cluster is +2 kJ/mol with respect to Int1a (see Int3a in Figs. 1a and 2). The thiol group sulfur atom interacts with the zeolitic proton ($H_aS = 2.21$ Å), whereas the thiol group hydrogen atom interacts with a Lewis base oxygen atom of the cluster ($H_1O_2 = 2.33$ Å).

3.2. Thiol Group Sulfur Removal

The second part of the desulfurization of DBT corresponds to sulfur atom removal, which is achieved through the elimination of the thiol group once sulfur is protonated by the zeolite proton. The geometry of the transition state is shown in Fig. 2 (see TS3a), where one notes that the breaking of the C–S bond has already been achieved in the transition state ($C_1S = 2.39$ Å in TS3a versus 1.81 Å in Int3a). This reaction leads to the formation of a phenoxy intermediate (see Int4a in Figs. 1b and 2). The phenoxy bond has not yet been formed in TS3a, but the H_2S molecule has already been formed (see Table 1). The activation energy barrier of this step is $E_{act} = 257$ kJ/mol with respect to Int3a (see Fig. 1b). Cleavage of the thiol C–S bond requires an activation energy that is lower than that of the DBT C–S bond cleavage (see Figs. 1a and 1b). This is in agreement with the experimental results for thiophenic derivative desulfurization (3, 4). Desulfurization of thiol compounds is more easily achieved than that of thiophenic polyaromatic compounds.

The phenoxy intermediate Int4a, though displaying a geometry very close to that of Int2a (see Fig. 2), is energetically more stable than Int2a (see Figs. 1a and 1b).

After adsorption of H_2 onto a Lewis base oxygen atom, H_2 dissociates, and this leads to the protonation and release of the phenoxy species, whereas an oxygen atom becomes protonated (see TS4a in Figs. 1b and 2). The geometry of this transition state is very similar to that of TS2a (see Table 1). Biphenyl is formed (see Int5a in Figs. 1b and 2). The activation energy barier that allows the formation of Int5a is $E_{act} = 306$ kJ/mol with respect to physisorbed biphenylthiol, and 277 kJ/mol with respect to Int4a. One notes that this strong stabilization of TS4a E_{act} with respect to TS2a E_{act} is consistent with the Polanyi–Brønsted relation (see Figs. 1a and 1b) (49).

3.3. Aromatic Hydrogenation

The other reaction route for DBT HDS is initiated by hydrogenation of one of the DBT aromatic rings (reaction b in Scheme 1) (3, 4). Zeolite catalysts are known to have hydrogenation capability. Senger and Radom (48) described the hydrogenation of a small olefin by H- and Na-exchanged zeolite clusters. Milas and Nascimento (47) analyzed the hydrogenation of isobutene by a H-zeolite cluster. Frash and Van Santen (50, 51) considered the case of olefin hydrogenation by Zn- and Ga-exchanged zeolite clusters. A hydrogenation mechanism similar to that of olefin is obtained for benzene (see Fig. 3).

After adsorption of benzene to the zeolite cluster proton in an η^2(CC) coordination mode (see Int1b in Figs. 3 and 4), benzene becomes protonated (24). H_2 coadsorbs with the activated (24) benzene molecule to the deprotonated cluster and dissociates (see TS1b in Figs. 3 and 4), and the H_2 hydrogen atoms move apart (see H_1H_2 in Table 2). One of the H atoms bonds to a zeolite cluster oxygen atom (see O_1H_1 in Table 2), and the other bonds to the benzene carbon atom next to the one that has been previously protonated (see H_2C_1 in Table 2). The other relevant geometric parameters of the transition state are summarized in Table 2. The activation energy barrier of benzene hydrogenation, which leads to the formation of cyclohexadiene, is $E_{act} = 229$ kJ/mol. Cyclohexadiene physisorbs to the acidic cluster (see Int2b in Fig. 4).

The hydrogenation transition state of cyclohexadiene has a geometry that is very close to that of TS1b (see TS2b in Table 2 and Fig. 4). However, the activation energy barrier for TS2b is much lower than that of the hydrogenation of benzene (E_{act} is 131 kJ/mol versus 229 kJ/mol). Furthermore, in contrast to TS1b, TS2b results in a strongly exothermic reaction. The product of cyclohexadiene hydrogenation (see Int3b in Figs. 3 and 4), that is, cyclohexene,

TABLE 2

Main Geometry Parameters of the Transition States in the Hydrogenation of Benzene Catalyzed by a T4 Acidic Zeolite Cluster[a]

	TS1b	TS2b	TS3b
AlO_1	1.81	1.79	1.78
O_1H_1	1.53	1.77	1.89
H_1H_2	0.84	0.79	0.77
H_2C_1	1.66	1.92	2.03
AlO_1H_1	104	99.2	108.2
$O_1H_1H_2$	167.7	169.6	169.8
$H_1H_2C_1$	137.6	131.9	95.6

[a] Distances in Å and angles in degrees. The labels that are used to design the transition states in this table are described in Fig. 4.

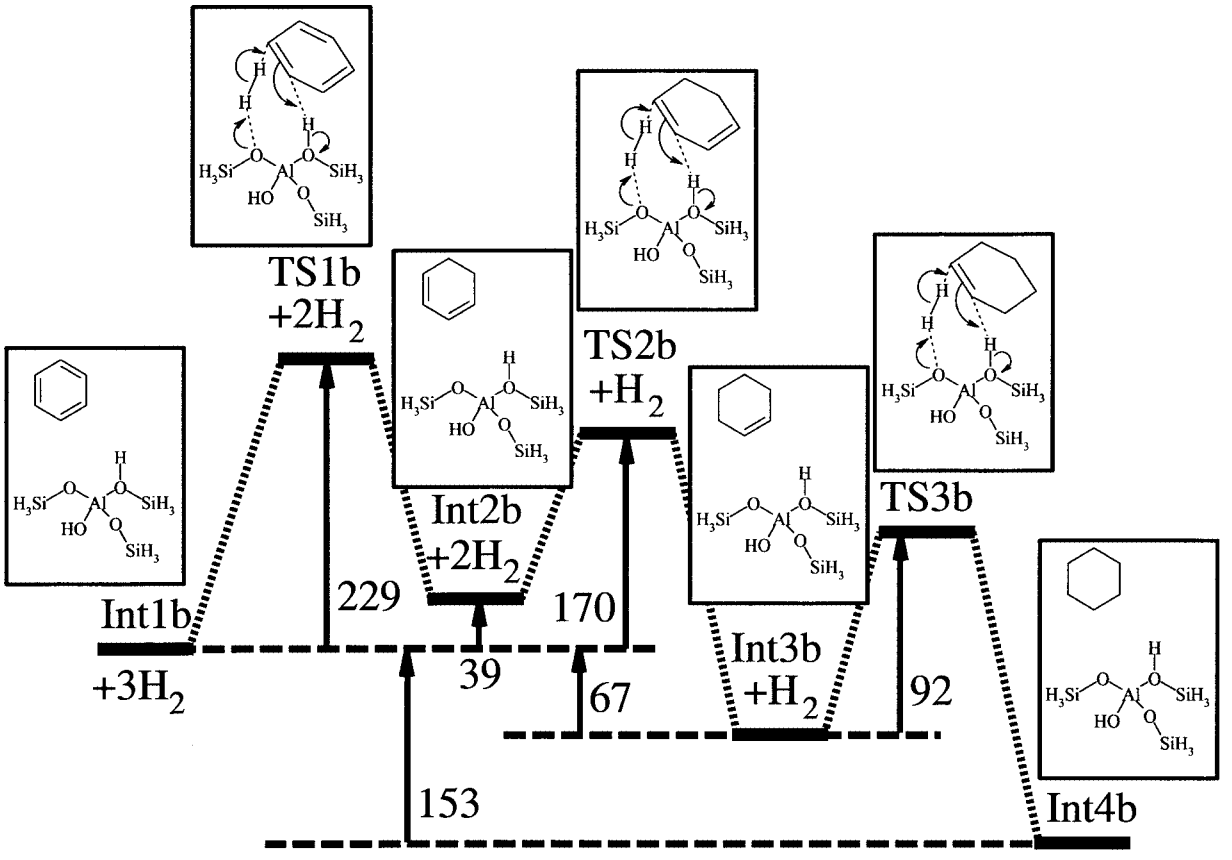

FIG. 3. Reaction energy diagram of benzene hydrogenation catalyzed by an acidic zeolitic cluster (in kJ/mol).

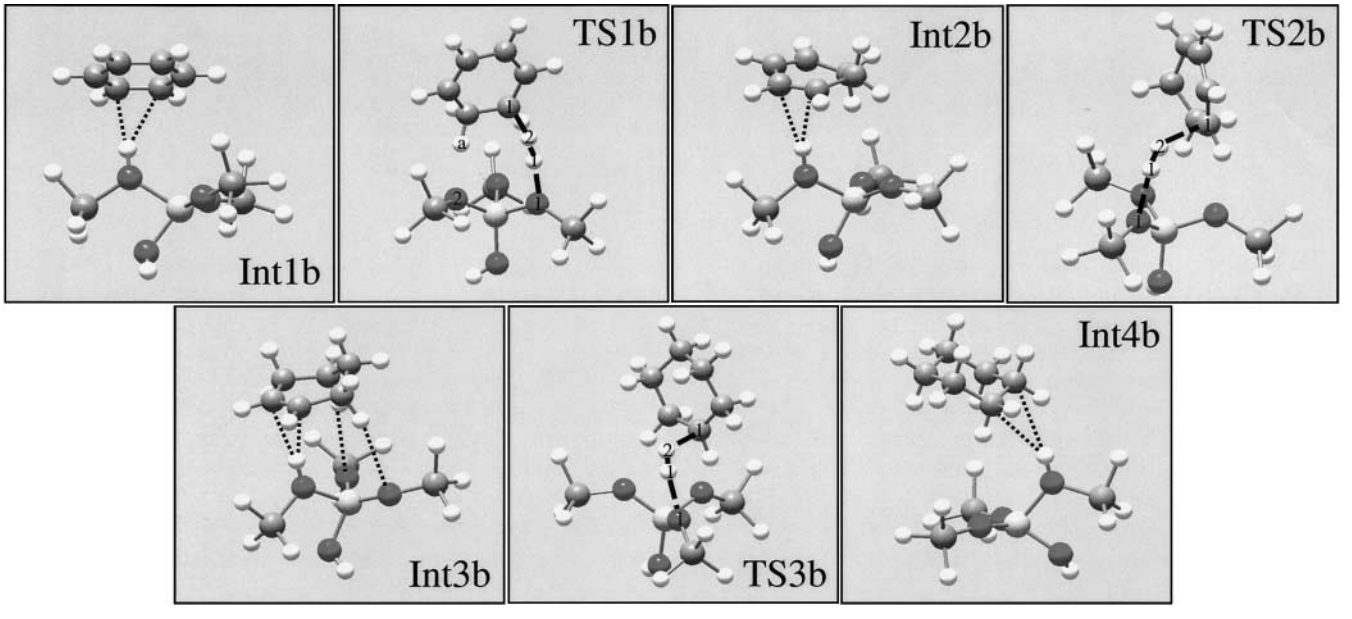

FIG. 4. Geometries of the intermediates and transition states in the hydrogenation of benzene.

is −106 kJ/mol below the energy level of Int2b. Benzene loses its aromaticity in TS1b, which explains why this reaction step is endothermic.

When hydrogenation continues, a similar trend is obtained. The activation energy barrier to achieving hydrogenation of cyclohexene is $E_{act} = 92$ kJ/mol. The geometry of the transition state is also very close to those of TS1b and TS2b (see TS3b in Fig. 4, and in Table 2). The energy of the product of this reaction is −86 kJ/mol with respect to Int3b. The geometry of cyclohexane physisorbed to the acidic cluster is shown in Fig. 4 (see Int4b).

The overall reaction energy diagram of benzene hydrogenation to cyclohexane can be seen in Fig. 3. Hydrogenation of benzene is a difficult step due to the loss of molecule aromaticity, but then hydrogenation becomes easier. Furthermore, as hydrogenation is exothermic, with the exception of benzene, it is likely that once cyclohexadiene is formed the reaction will continue readily to cyclohexane.

Benzene has been used as an approximate model of DBT for the study of hydrogenation. We showed in a previous study of aromatic isomerization that toluene could be used as a very good model for dimethyldibenzothiophene, methyldibenzothiophene, or methylbenzothiophene (19). The present results agree with the experimental observations of DBT hydrogenation (1–12). It is predicted that as soon as hydrogenation is initiated on an aromatic ring it will continue until the full ring is hydrogenated. It should be noted that benzene hydrogenation is more favorable than either the cracking of DBT, or the sulfur removal of biphenylthiol. We will now analyze how DBT hydrogenation affects the cracking reaction.

3.4. *Hexahydrodibenzothiophene Cracking*

Once hydrogenated, the DBT molecule is desulfurized via a succession of mechanisms similar to those obtained previously (see Figs. 1a, 1b, and 5). Hexahydrodibenzothiophene physisorbs to the zeolitic proton (reaction c in Scheme 1; see Int1c in Figs. 5 and 6). The molecule adopts an η^1(S) coordination mode with respect to the proton ($H_aS = 2.17$ Å, and $H_aO_1 = 1.00$ Å).

The C–S bond cleavage transition state is different from that obtained for DBT (see TS1c in Fig. 6). Here, the carbocationic nature of the transition state is revealed, and structure close to a secondary carbenium ion can be observed ($C_1C_2C_3H_3 = -5.7°$). The C–S bond cleavage shows an earlier stage transition state. The CS distance is 3.11 Å, but a hydrogen atom is located between the sulfur atom and the carbon atom ($SH_2 = 2.26$ Å). The protonation of the sulfur atom has not yet been reached ($O_1H_a = 1.05$ Å) and $H_aS = 1.94$ Å). Similarly, the alkoxy bond between the zeolite oxygen atom O_3 and the carbon atom C_1 has not yet been formed ($O_3C_1 = 2.94$ Å). The activation energy barrier for TS1c is $E_{act} = 235$ kJ/mol. This value is very close to those of the activation energy barriers that are required for the cracking of thiophene, dihydrothiophene,

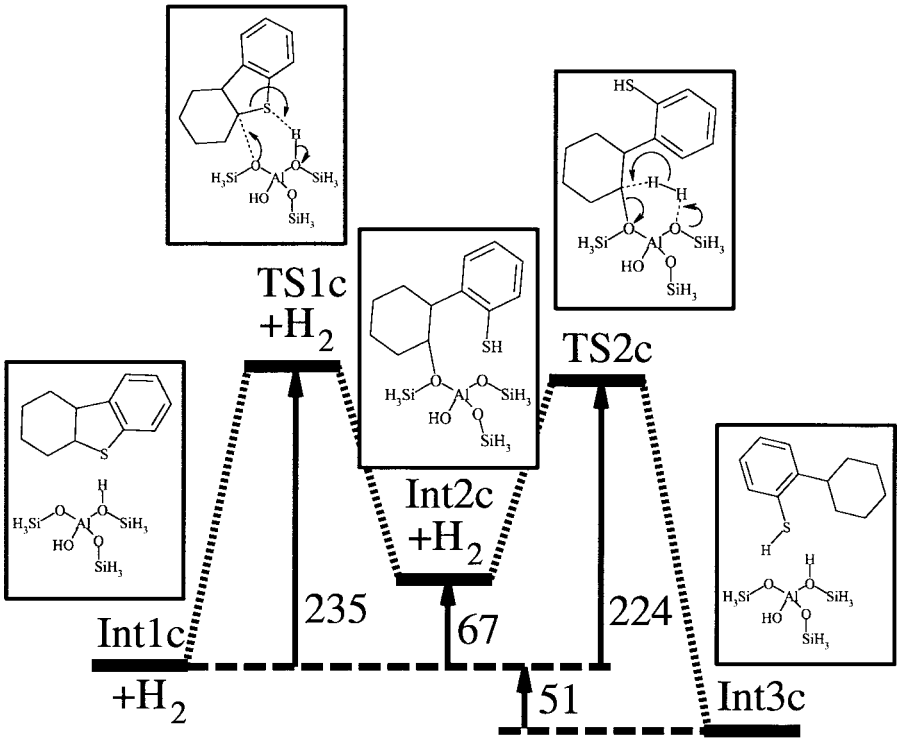

FIG. 5. Reaction energy diagram of thiophenic ring cracking of benzocyclohexanothiophene catalyzed by an acid zeolitic cluster (in kJ/mol).

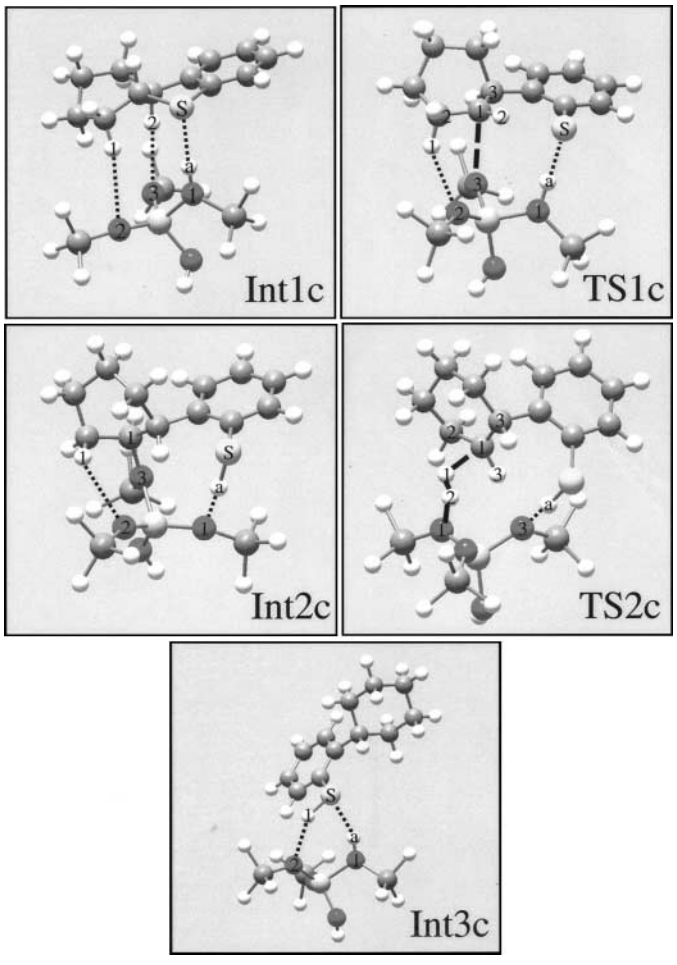

FIG. 6. Geometries of the intermediates and transition states in the thiophenic ring cracking and desulfurization of hydrogenated DBT.

and tetrahydrothiophene (14), and represents a strong energy decrease in comparison to that of DBT cracking (E_{act} is 235 kJ/mol versus 288 kJ/mol).

The cycloalkoxy species that is formed is more stable than the DBT phenoxy intermediate Int2a (see Int2c in Figs. 5 and 6). This is an expected result, as phenoxy intermediates are not observed experimentally, whereas alkoxy intermediates are (52, 53). The difference between the Int2c and Int1c energies is +67 kJ/mol. The alkoxy bond is $C_1O_3 = 1.48$ Å. Additional O···H short distances help with the stabilization of Int2c ($H_1O_2 = 2.77$ Å, $H_aO_1 = 2.24$ Å, and $O_2H_2 = 2.72$ Å). The thiophenic ring hydrogenation effect on the energy of the intermediate next to the cracking TS has also been observed in the case of thiophene (14).

H_2 adsorbs, and the back-protonation of the zeolitic cluster and protonation and release of the alkoxy species take place. The geometry of the transition state is shown in Fig. 6 (see TS2c). The breaking of the C–O bond and the protonation of the carbon atom were associative mechanisms in TS2a. Here, only the protonation mechanisms can be seen in the TS ($C_1O_3 = 3.13$ Å, and $C_1C_2C_3H_3 = 8.2°$). The dissociating H_2 molecule has a similar geometry in TS2c and in TS2a ($C_1H_1 = 1.94$ Å, $H_1H_2 = 0.78$ Å, $O_1H_2 = 1.82$ Å, $O_1H_2H_1 = 172.0°$, and $H_2H_1C_1 = 112.1°$). The activation energy barrier is $E_{act} = 157$ kJ/ml with respect to Int2c. The energy stabilization of the hydrogenation step compared to that of DBT is very large ($\Delta E_{act} \approx 130$ kJ/mol).

TS2c leads to the formation of cyclohexyl-2-benzenethiol (see Int3c in Figs. 5 and 6). We defined this system, so that the molecule would be in an η^1(S) coordination mode with respect to the acidic proton ($SH_a = 2.25$ Å, $H_1O_2 = 2.25$ Å, and $H_2O_2 = 2.78$ Å). This system is thermodynamically favored.

Comparison of the reaction energy diagrams of the thiophenic ring cracking of DBT (see Fig. 1a) with those of hexahydrodibenzothiophene (see Fig. 5) shows the magnitude of the effect of hydrogenation on one DBT benzo ring. All intermediates and transition states along the reaction pathway are more stable for hydrogenated DBT. The more significant change concerns the hydrogenation step of the alkoxy species. Presumably, the hydrogenation of both DBT benzo rings is not significant, as observed in dihydrothiophene and tetrahydrothiophene cracking (14). The cracking of hydrogenated DBT appears to be as difficult to achieve as the benzene hydrogenation reaction. This could explain why hydrogenation of DBT has been experimentally observed to occur only on one of the DBT rings (1–8).

4. CONCLUSIONS

In this theoretical study, we showed that unpromoted acidic zeolites can catalyze the hydrodesulfurization of DBT, although it is a demanding process (9–15). Two different parallel reaction routes are possible: the direct desulfurization of DBT and the hydrogenation of a benzo ring prior to sulfur removal.

The elementary DBT cracking reaction, which leads to the formation of biphenylthiol, is the most difficult reaction in the DBT desulfurization reaction pathway. Once this step has been achieved, sulfur removal becomes favorable. When the activation energies of this reaction are compared to those of the sulfur removal reaction, one can conclude that it is unlikely that biphenylthiol follows the thiophenic ring closure reaction pathway. The reverse reaction of desulfurization, which gives biphenylthiol from biphenyl and H_2S, appears to have the largest activation energies and is therefore not favorable. The formation of DBT from biphenyl and H_2S following the reaction pathways as described in this study is extremely unlikely to occur.

Benzene hydrogenation, which has been assumed to be a model for the hydrogenation of one DBT benzo ring, is a more favorable reaction than either DBT cracking or biphenylthiol desulfurization. No competition between

hydrogenation and dehydrogenation of benzene is predicted, and hydrogenation will carry on until the full aromatic ring has been hydrogenated. The most difficult step in the benzene reaction to cyclohexane is the first hydrogenation reaction step. Then, the activation energies of hydrogenation of hydrogenated benzene are around 100 kJ/mol below those required to achieve hydrogenation of benzene.

The effect of the hydrogenation of a benzo ring of DBT is very significant in thiophenic ring cracking. The ring cracking activation energies of hydrogenated DBT are on the same order as that of aromatic hydrogenation activation energies. Once a benzo ring has been hydrogenated, the reaction route that will likely be followed is thiophene ring cracking. In all circumstances, the hydrogenated DBT ring closure activation energies are too high, and this reaction does not compete with the others.

ACKNOWLEDGMENTS

Computational resources were partly granted by the Dutch National Computer Facilities (NCF). This work was performed within the European Research Group, "Ab Initio Molecular Dynamics Applied to Catalysis," supported by the Centre National de la Recherche Scientifique (CNRS), the Institut Français du Pétrole (IFP), and the TotalFinaElf Raffinage Distributions company. XR and XS thank TotalFina Raffinage Distributions for financial support.

REFERENCES

1. Knudsen, K. G., Cooper, B. H., and Topsøe, H., *Appl. Catal. A* **189**, 205 (1999).
2. Weber, T., Prins, R., and Van Santen, R. A., *in* "Transition Metal Sulphides, Chemistry and Catalysis," Vol. 60. NATO ASI Series 3. Kluwer Academic Publishers, Dordrecht, 1998.
3. Landau, M. V., *Catal. Today* **36**, 393 (1997).
4. Landau, M. V., Berger, D., and Herskowitz, M., *J. Catal.* **158**, 236.
5. Michaud, P., Lemberton, J. L., and Pérot, G., *Appl. Catal. A* **169**, 343 (1998).
6. Meille, V., Schulz, E., Lemaire, M., and Vrinat, M., *J. Catal.* **170**, 29 (1997).
7. Singhal, G. H., Espino, R. L., and Sobel, J. E., *J. Catal.* **67**, 446 (1981).
8. Vasudevan, P. T., and Fierro, J. L. G., *Catal. Rev.–Sci. Eng.* **38**(2), 161 (1996).
9. Vrinat, M. L., Gachet, C. G., and De Mourgues, L., *in* "Catalysis by Zeolites" (B. Imelik, C. Naccache, Y. Ben Taarit, J. C. Vedrine, G. Coudurier, and H. Praliaud, Eds.), p. 19. Elsevier, Amsterdam, 1980.
10. Cid, R., Orellana, F., and Agudo, A. L., *Appl. Catal.* **32**, 327 (1987).
11. Welters, W. J. J., De Beer, V. H. J., and Van Santen, R. A., *Appl. Catal. A* **119**, 253 (1994).
12. Welters, W. J. J., Vorbeck, G., Zandbergen, H. W., De Haan, J. W., De Beer, V. H. J., and Van Santen, R. A., *J. Catal.* **150**, 155 (1994).
13. Saintigny, X., Van Santen, R. A., Clémendot, S., and Hutschka, F., *J. Catal.* **183**, 107 (1999).
14. Rozanska, X., Van Santen, R. A., and Hutschka, F., *J. Catal.* **200**, 79 (2001).
15. Yu, S. Y., Li, W., and Iglesia, E., *J. Catal.* **187**, 257 (1999).
16. Van Santen, R. A., and Kramer, G. J., *Chem. Rev.* **95**, 637 (1995).
17. Sauer, J., *in* "Cluster Models for Surface and Bulk Phenomena: Proceedings of a NATO Advanced Research Workshop" (G. Pacchioni, P. S. Bagus, and F. Parmigiani, Eds.), p. 533. Plenum, London, 1992.
18. Van Santen, R. A., De Bruyn, D. P., Den Ouden, C. J. J., and Smit, B., *in* "Introduction to Zeolite Science and Practice" (H. van Bekkum, E. M. Flaningen, and J. C. Jansen, Eds.), Vol. 58, p. 317. Elsevier, Amsterdam, 1991.
19. Rozanska, X., Saintigny, X., Van Santen, R. A., and Hutschka, F., *J. Catal.* **202**, 141 (2001).
20. Vollmer, J. M., and Truong, T. N., *J. Phys. Chem. B* **104**, 6308 (2000).
21. Boronat, M., Viruela, P., and Corma, A., *J. Phys. Chem. A* **102**, 982 (1998).
22. Sierka, M., and Sauer, J., *J. Phys. Chem. B* **105**, 1603 (2001).
23. Vos, A. M., Rozanska, X., Schoonheydt, R. A., Van Santen, R. A., Hutschka, F., and Hafner, J., *J. Am. Chem. Soc.* **123**, 2799 (2001).
24. Rozanska, X., Van Santen, R. A., Hutschka, F., and Hafner, J., *J. Am. Chem. Soc.* **123**, 7655 (2001).
25. Van Santen, R. A., and Rozanska, X., *in* "Advances in Chemical Engineering" (J. Wei, J. H. Seinfeld, M. M. Denn, G. Stephanopoulos, A. Chakraborty, J. Ying, and N. Peppas, Eds.), Vol. 28, p. 399. Academic Press, New York, 2001.
26. Zhen, S., and Seff, K., *Microporous Mesoporous Mater.* **39**, 1 (2000).
27. Sato, K., Nishimura, Y., Honna, K., Matsubayashi, N., and Shimada, H., *J. Catal.* **200**, 288 (2001).
28. Frisch, M. J., Trucks, G. W., Schlegel, H. B., Scuseria, M. A., Robb, M. A., Cheeseman, J. R., Zakrzewski, V. G., Montgomery, J. A., Stratmann, R. E., Burant, J. C., Dapprich, S., Millam, J. M., Daniels, A. D., Kudin, K. N., Strain, M. C., Farkas, O., Tomasi, J., Barone, V., Cossi, M., Cammi, R., Mennucci, B., Pomelli, C., Adamo, C., Clifford, S., Ochterski, J., Petersson, G. A., Ayala, P. Y., Cui, Q., Morokuma, K., Malick, D. K., Rabuck, D. K., Raghavachari, K., Foresman, J. B., Cioslowski, J., Ortiz, J. V., Stefanov, B. B., Liu, G., Liashenko, A., Piskorz, P., Komaromi, I., Gomperts, R., Martin, R. L., Fox, D. J., Keith, T., Al-Laham, M. A., Peng, C. Y., Nanayakkara, A., Gonzales, C., Challacombe, M., Gill, P. M. W., Johnson, B. G., Chen, W., Wong, M. W., Andress, J. L., Head-Gordon, M., Replogle, E. S., and Pople, J. A., "Gaussian 98," revision A. 1. Gaussian, Inc., Pittsburgh PA, 1998.
29. Becke, A. D., *Phys. Rev. A* **38**, 3098 (1988).
30. Lee, C., Yang, W., and Parr, R. G., *Phys. Rev. B* **37**, 785 (1988).
31. Becke, A. D., *J. Chem. Phys.* **98**, 5648 (1993).
32. Zygmunt, S. A., Mueller, R. M., Curtiss, L. A., and Iton, L. E., *J. Mol. Struct.* **430**, 9 (1998).
33. Civalleri, B., Garrone, E., and Ugliengo, P., *J. Phys. Chem. B* **102**, 2373 (1998).
34. Boys, S. F., and Bernardi, F., *Mol. Phys.* **19**, 553 (1970).
35. Van Duijneveldt, F. B., *in* "Molecular Interactions: From Van der Waals to Strongly Bound Complexes" (S. Scheiner, Ed.), p. 81. Wiley, New York, 1997.
36. Lendvay, G., and Mayer, I., *Chem. Phys. Lett.* **297**, 365 (1998).
37. Jacobs, P. A., and Martens, J. A., *in* "Introduction to Zeolite Science and Practice" (H. van Bekkum, E. M. Flaningen, and J. C. Jansen, Eds.), Vol. 58, p. 445. Elsevier, Amsterdam, 1991.
38. Maxwell, I. E., and Stork, W. H. J., *in* "Introduction to Zeolite Science and Practice" (H. van Bekkum, E. M. Flaningen, and J. C. Jansen, Eds.), Vol. 58, p. 571. Elsevier, Amsterdam, 1991.
39. Garcia, C. L., and Lercher, J. A., *J. Mol. Struct.* **293**, 235 (1993).
40. Geobaldo, F., Palomino, G. T., Bordiga, S., Zecchina, A., and Areán, C. O., *Phys. Chem. Chem. Phys.* **1**, 561 (1999).
41. Hoffman, R. W., *in* "Dehydrobenzene and Cycloalkynes," p. 317. Academic Press, New York, 1967.
42. Reinecke, M. G., and Del Mazza, D., *J. Org. Chem.* **54**, 2142 (1989).

43. Kristyan, S., and Pulay, P., *Chem. Phys. Lett.* **229**, 175 (1994).
44. Sauer, J., Ugliengo, P., Garrone, E., and Saunders, V. R., *Chem. Rev.* **94**, 2095 (1994).
45. Lein, M., Dobson, J. F., and Gross, E. K. U., *J. Comput. Chem.* **20**, 12 (1999).
46. Pelmenschikov, A., and Leszczynski, J., *J. Phys. Chem. B* **103**, 6886 (1999).
47. Milas, I., and Nascimento, M. A. C., *Chem. Phys. Lett.* **338**, 67 (2001).
48. Senger, S., and Radom, L., *J. Am. Chem. Soc.* **122**, 2613 (2000).
49. Van Santen, R. A., *J. Mol. Catal. A* **115**, 405 (1997).
50. Frash, M. V., and Van Santen, R. A., *J. Phys. Chem. A* **104**, 2468 (2000).
51. Frash, M. V., and Van Santen, R. A., *Phys. Chem. Chem. Phys.* **2**, 1085 (2000).
52. Paukshtis, E. A., Malysheva, L. V., and Stepanov, V. G., *React. Kinet. Catal. Lett.* **65**, 145 (1998).
53. Song, W., Nicholas, J. B., and Haw, J. F., *J. Am. Chem. Soc.* **123**, 121 (2001).